Article

Not peer-reviewed version

Cellular Response of Adapted and Non-Adapted *Tetrahymena thermophila* Strains to Europium Eu(III) Compounds

Patricia Alonso , Javier Blas , Francisco Amaro , Patricia De Francisco , Ana Martin-Gonzalez , Juan Carlos Gutiérrez *

Posted Date: 19 March 2024

doi: 10.20944/preprints202403.1161.v1

Keywords: Europium; lipid metabolism; bioaccumulation; oxidative stress; gene expression; Tetrahymena thermophila

Article

Cellular Response of Adapted and Non-Adapted *Tetrahymena thermophila* Strains to Europium Eu(III) Compounds

Patricia Alonso, Javier Blas, Francisco Amaro, Patricia de Francisco, Ana Martín-González and Juan Carlos Gutiérrez *

Department of Genetics, Physiology and Microbiology, Faculty of Biology, Complutense University of Madrid, 28040 Madrid, Spain
* Correspondence: juancar@bio.ucm.es

Simple Summary: The analysis of the toxicity of lanthanides, and among them europium, has grown in recent years due to its multiple applications in different human technologies. In the present research work, we analyze its toxicity in the eukaryotic microorganism model *Tetrahymena thermophila*, comparing strains adapted to high concentrations of two europium compounds (chloride and oxide forms) with the wild type strain. The oxidative stress caused by europium oxide is reduced by overexpression of genes encoding various antioxidant enzymes. Likewise, metallothionein genes of this microorganism are overexpressed, which could indicate the potential chelation of this lanthanide by these proteins. Lipid metabolism and autophagy are involved in the cellular stress response to europium. Both bioaccumulation in vacuoles, and their subsequent expulsion, as well as a possible biotransformation to europium phosphate are involved in the europium detoxification process in these cells. A better understanding of the cellular mechanisms of lanthanide detoxification is very useful information for solving bioremediation problems and possible intoxications in animals and humans.

Abstract: Europium is one of the most reactive lanthanides and humans use it in many different applications, but we still know little about its potential toxicity and cellular response to its exposure. Two strains of the eukaryotic microorganism model *Tetrahymena thermophila* adapted to high concentrations of two Eu(III) compounds ($EuCl_3$ or Eu_2O_3) were obtained and compared to a control strain and cultures treated with both compounds. In this ciliate, $EuCl_3$ is more toxic than Eu_2O_3. LC_{50} values show that this microorganism is more resistant to these Eu(III) compounds than other microorganisms. Oxidative stress originated mainly by Eu_2O_3 is minimized by overexpression of genes encoding important antioxidant enzymes. The overexpression of metallothionein genes under treatment with Eu(III) compounds supports the possibility that this lanthanide may interact with the -SH groups of the cysteine residues from metallothioneins and/or displace essential cations of these proteins during their homeostasis function. Both lipid metabolism (lipid droplets that fuse with europium-containing vacuoles) and autophagy are involved in the cellular response to europium stress. Bioaccumulation, together with a possible biomineralization to europium phosphate, seems to be the main mechanism of Eu(III) detoxification in these cells.

Keywords: europium; lipid metabolism; bioaccumulation; oxidative stress; gene expression; *Tetrahymena thermophila*

 doi:10.20944/preprints202403.1161.v1

Graphical Abstract

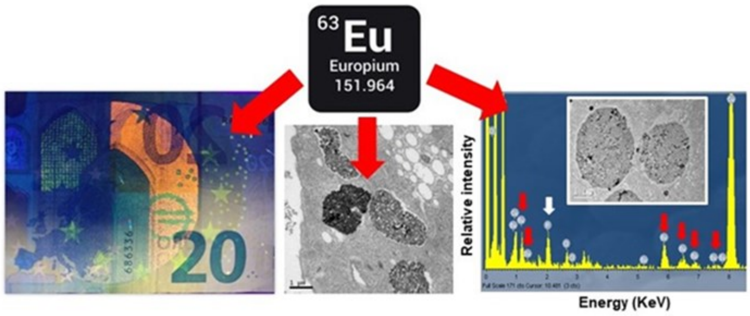

1. Introduction

In the last decade, there has been growing interest in the potential toxicity of lanthanides (Ln), due to their extensive human use in many recent technologies [1–5]. Some of which are: electronic devices (television screens, computers, cell phones, silicon chips, monitor displays, long-life rechargeable batteries, camera lenses, light emitting diodes (LEDs), etc.), manufacturing (ceramic pigments, colorants in glassware, chemical oxidizing agents and automotive catalytic converters) and renewable energies (solar cells, hybrid automobiles, wind turbines and biofuels catalysis) [6,7]. In addition, they have a special interest in biomedical applications, for instance: nuclear medicine imaging, phototherapy in tumor therapy, magnetic resonance, and as fluorescent probes in optical cellular imaging [6,8–10]. Ln have also been used as fertilizers in oriental agriculture. About 50 to 100 tons of Ln oxides have been used in Chinese agriculture each year [11]. Moreover, because of agricultural and industrial activity, Ln have been detected in wastewater and aquatic ecosystems. Likewise, Ln has been used as a feed supplement to promote the growth of farm animals, and this has favored the presence of Ln in soil through animal wastes [2,12,13]. Several studies indicate the potential health risks for humans from this Ln pollution by two main ways, direct by occupational exposure and indirect by ingestion of water or foods containing these pollutants because of farming [5,14–16].

In the periodic table, lanthanides group 15 metals, which together with yttrium (Y) and scandium (Sc) constitute the so-called rare earth elements (REEs). The term "rare" does not mean that they are scarce in the earth's crust, for example, cerium (Ce) is about 100 times more abundant than cadmium (Cd), one of the most toxic metals. Despite the important risks for ecosystems and/or organisms as stated by many authors, the ecotoxicological studies to assess the REE toxicity of these emerging pollutants are still scarce. Many of these studies are focused exclusively on a few REEs, particularly Gadolinium (Gd), Lanthanum (Ln) and Cerium (Ce) [1,4,12,15,17]. Most of them mainly analyze their effects on cell growth and viability, with a lower knowledge on molecular, physiological, and cell structural effects.

Europium (Eu) is a Ln relatively rare in the earth's crust (an average of 2 - 2.2 ppm), not found as a free element but as part of many minerals. Like other Ln its predominant oxidation state is +3, but it can easily form divalent (+2) compounds, which is unusual for other lanthanides. Eu is the most reactive of all REEs [12]. It is one of the chemical elements that form fluorescent compounds that are used in devices such as color televisions, fluorescent lamps, LEDs (light-emitting diodes), LCD screens and many lighting system. Europium oxide (Eu2O3) is widely used as a fluorescent element in television sets [7–9,18,19]. Other uses of Eu include: a)- the European Union uses Eu in the ink of euro bills, to prevent counterfeiting. Depending on the molecule of which it is a part, Eu can emit red, green, or blue light. Under special laser or ultraviolet light (UV), the outline of Europe on the bills shines greenish, the crown of stars is yellow or red, and the monuments, signatures and hidden seals are dark blue. An example is shown in the graphical abstract (an image of a 20 € bill under UV light), b)- in astrophysics, the Eu signature from the light spectrum emitted by a star can be used to classify stars [20].

Preprints.org (www.preprints.org) | NOT PEER-REVIEWED | Posted: 19 March 2024 doi:10.20944/preprints202403.1161.v1

Compared to other metals, Eu does not exhibit considerable toxicity in both its chloride and oxide forms, although it is slightly more toxic in its nitrate form [16]. Its toxicity as $EuCl_3$ salt is like other REEs, having been shown to be quite harmful during early life stages in sea urchins [21]. Toxicity of Eu hydroxide nanoparticles in mice is low even at high concentrations [22]. For humans, prolonged exposure to Eu vapors can be very dangerous, causing pulmonary embolisms, and can be a danger to the liver when it accumulates in the body [5].

Due to the increasing demand for rare earth metals by modern human technologies, their possible bioaccumulation by microorganisms, such as bacteria, has been studied [23]. The thermophilic bacterium *Thermus scotoductus* has shown a high capacity to tolerate high Eu concentrations, biomineralize it and bioaccumulate it intra- and extracellularly [24]. Likewise, biosorption has been considered as a non-costly and environmentally friendly mechanism to recover REEs from industrial electronic waste [25]. Good results have been obtained in studies to recover Eu(III) and other Ln using microalgae [26], bacteria [27,28], filamentous fungi [29] or yeasts [30]. The ciliate protozoan *Paramecium* sp. can transform aqueous inorganic forms of Eu(III), Pb(II) or U(VI) to organic complexes by binding to glycoproteins present in the ciliate coat, initiating this process as a biosorption mechanism [31].

Tetrahymena thermophila is an eukaryotic microorganism (ciliate-model) widely used in ecotoxicological studies [32–38], because it has an animal biology and more orthologous genes with humans than other eukaryotic microorganisms (such as yeasts). Among 874 human orthologous genes present in *T. thermophila*, 58 are related to human diseases [39]. Therefore, *T. thermophila* is an excellent eukaryotic model for comparative ecotoxicological analysis with higher organisms, including humans.

In the present study, two strains of the ciliate *T. thermophila* adapted to high concentrations of $EuCl_3$ or Eu_2O_3 were obtained and compared with the control strain. The toxicity levels of both Eu(III) compounds, and how they affect the growth of the ciliate, have been studied. An analysis of the oxidative stress induction by these Eu compounds has been carried out. Likewise, the bioaccumulation capacity of Eu by these adapted strains has been also studied by transmission electron microscopy (TEM) and microanalysis (TEM-XEDS). In addition, the expression of nine different genes encoding antioxidant enzymes, together with four general stress genes (encoding metallothioneins) have been analyzed by qRT-PCR in both Eu-adapted strains. All these analyses together give us a general overview of the cellular stress response to Eu in this eukaryotic microorganism.

2. Materials and Methods

2.1. Microorganism, Culture Conditions and Eu-Adapted Strains

Dr. E. Orias (University of California, USA), kindly supplied the *Tetrahymena thermophila* strain SB1969. This ciliate was axenically grown in PP210 medium (as described in [40]), and cell cultures were maintained at a constant temperature of 30 ± 1ºC. The Eu(III) compounds used were: europium chloride ($EuCl_3$) (Acrosorganics) and europium oxide (Eu_2O_3) (Aldrich Chemistry).

In all experiments with *T. thermophila* growing in PP210 medium, aqueous solutions of $EuCl_3$ (2 mM) were used, while Eu_2O_3 (4 mM) was used in aqueous solution containing 53.6% 1 N HCl. Both concentrations correspond to approximately half of the LC_{50} values obtained for each Eu compound. Experiments performed in Tris-HCl buffer were carried out from a culture previously grown (48h or late exponential phase) in PP210, and subsequently resuspended in 0.01 M Tris-HCl buffer (pH 7.5), after centrifugation (2,400 rpm, 2 min) of the culture grown in PP210.

The adaptation process to $EuCl_3$ or Eu_2O_3, which lasted about 8 months, consisted of gradually exposing strain SB1969 to increasing concentrations of each Eu compound, until the maximum tolerated concentration (MTC) was reached. In this way, cells adapted to a very high $EuCl_3$ (5.5 mM) (Tt$EuCl_3$-adap strain) or Eu_2O_3 (8.5 mM) (TtEu_2O_3-adap strain) concentrations were selected and both strains were maintained over time in PP210 medium in the constant presence of the Eu(III) compounds at the corresponding MTC.

2.2. Growth Kinetics and LC_{50} Calculation by Flow Cytometry

Growth curves were obtained for the three strains (control, $TtEuCl_3$-adap and $TtEu_2O_3$-adap) by counting cells in a Neubauer chamber from aliquots of the different cultures at different times. Subsequently, using the informatics application DMFit (http://browser.combase.cc/DMFit.aspx), growth curves were constructed according to the model proposed by [41]. The two parameters obtained from the growth curves were the specific growth rate (or speed) μ (h^{-1}) and the generation time Tg (h).

Flow cytometry was used to calculate cell mortality and LC_{50} values for Eu treatments. Samples were prepared from control cultures (100 ml) after reaching the end of the exponential phase (1-3 x 10^5 cells/ml). Cells were centrifuged (2,400 rpm, 2 min) and washed twice with 0.01M Tris-HCl buffer (pH 7.5). Two of the samples were resuspended in TrisHCl buffer and two others in PP210 medium. All these samples were treated with increasing concentrations of europium ($EuCl_3$ or Eu_2O_3), at 30 °C for 24 h. Each test was repeated three times to corroborate the results. LC_{50} values were estimated by using Probit analysis with Statgraphics Centurion XVI and STATA 9 (confidence 95 %, $p < 0.05$) as described in [42]. Cell mortality was estimated by adding to the cell suspension the fluorophore propidium iodide (PI) (Sigma) at a final concentration of 2.5 μg/ml. PI only penetrates and stains membrane-damaged cells (dead or severely damaged cells) [43]. Therefore, non-viable cells can be identified as PI-positive and quantified by fluorescence at 670 nm Lp (long pass) in the FL3 channel. The flow cytometer used was FACScalibur (Becton & Dickinson), equipped with an argon-ion excitation laser (488 nm). Three types of controls were used: 1- blank-sample: cells not exposed to metal and without PI, which allows calibrating the cytometer and detecting autofluorescence from the sample. 2- negative or live control: cells not exposed to metal but treated with PI, to evaluate basal mortality, and 3- positive or dead control: cells fixed with formaldehyde (37%) and treated with PI, to check the proper functioning of the cytometer.

2.3. Oxidative Stress Detection

To elucidate whether Eu compounds induce cellular production of peroxide radicals, the fluorochrome 2'-7'dichlorodihydrofluorescein diacetate (DA-DCDH2F) (Sigma) was used, which is incorporated into cells and subsequently, by the action of esterases, converted to DCDH2F (which is non-fluorescent). However, if free radicals are present it is rapidly oxidized to 2'-7'dichlorofluorescein (DCF) which is highly fluorescent (absorbs at a wavelength of approximately 485-500 nm and emits between 515-530 nm). This molecule is quite specific for peroxides (including hydrogen peroxide), peroxinitrite and hydroxyl radical detection but cannot detect superoxide anions [44]. In addition to the cultures treated with the Eu compounds, a positive control was performed by exposing the cells to the oxidizing agent menadione (MD) (Sigma) at a final concentration 2 mM for 30 min [45]. Fluorescence emission was quantified by flow cytometry.

2.4. Transmission Electron Microscopy (TEM) and Microanalysis (TEM-XEDS)

For ultrastructural analysis (TEM), both Eu-adapted strains ($TtEuCl_3$-adap and $TtEu_2O_3$-adap), a culture treated (1 or 24h) with $EuCl_3$ (2 mM), and a control (untreated) culture were chosen. All cellular samples were processed according to the protocol described in [46]. Briefly, after fixation and dehydration, the samples were embedded in Embed 812 resin (TAAB), following the manufacturer's instructions. The ultrathin sections, after contrasting with uranyl acetate (2% in distilled water) and Reynolds solution (lead citrate), were observed in a JEM 1010 (JEOL) transmission electron microscope at 80 Kv, and the images were captured with a Megaview II camera.

To analyze the elemental composition of the vacuolar electrodense deposits observed by TEM the $TtEuCl_3$-adapted strain was selected, and a microanalysis was performed using TEM-XEDS. Cells were fixed with glutaraldehyde (2.5%), washed with cacodylate buffer, dehydrated, and embedded in resin similar to the protocol used for TEM. Thin sections (1 μm) were observed under the JEM 2100HT electron microscope (JEOL) at 200 Kv, which incorporates an XEDS (X-Ray Energy Dispersive Spectroscopy) microanalysis system (Oxford, INCA).

Preprints.org (www.preprints.org) | NOT PEER-REVIEWED | Posted: 19 March 2024 doi:10.20944/preprints202403.1161.v1

2.5. Total RNA Isolation and cDNA Synthesis

Exponential cell cultures (1-3 x 10^5 cells/ml) from control, $EuCl_3$ treated (24h) culture and Eu-adapted cultures (constantly exposed to Eu compounds at each corresponding MTC) were harvested by centrifugation at 2,400 rpm for 2 min. Total RNA samples were isolated by using the TRIzol Reagent® method (Molecular Research Center, Inc.). RNA samples were treated with DNase I (Roche) for 30 min at 37ºC. RNA integrity was tested by agarose (1.2%) gel electrophoresis and sample concentrations were calculated spectrophotometrically by the NanoDrop 1000 (Thermo Scientific). First strand cDNA synthesis from total RNA (3 µg) was carried out using the commercial 1st Strand cDNA Synthesis kit for RT-PCR (AMV) (Roche) and oligo(dT)-adaptor primer (Roche). The retrotranscription reactions were performed in a Mastercycler gradient thermocycler (Eppendorf), following this temperature program: 10 min at 25ºC, 60 min at 42ºC and 5 min at 99ºC.

2.6. Quantitative RT-PCR (qRT-PCR)

cDNA samples were amplified in duplicated in 96 wells microtiter plates. Each qRT-PCR reaction (20 µl) contained: 2 µl of a 10-1 dilution of the corresponding cDNA sample and 18 µl of a master mix, consisting of SYBR Green 1x (Takara), the Rox 1x dye (Takara), which is used to normalize fluorescence intensity, sterile water and the previously designed primer pair for each selected gene (0.2 µM). PCR primers (Table S1) were designed using the "Primer Quest and Probe Design" online application from IDT (Integrated DNA Technologies, https://eu.idtdna.com/PrimerQuest/Home/Index), and synthetized by the commercial companies Invitrogen or IDT. Beta-actin gene (*TtACT*) was used as an endogenous control or normalizer gene, as it has been validated as a reference gene in qRT-PCR under either biotic or abiotic stresses [47]. Melting curves were obtained and primers specificity was tested by confirming each PCR product (amplicon) by gel electrophoresis and sequencing. Real-time PCR reactions were carried out in an iQ5 real-time PCR apparatus (Bio-Rad) and the thermal cycling protocol was as follows: 5 min at 95ºC, 40 cycles (30 s at 95ºC, 30 s at 55º C and 20 s at 72º C), 1 min at 95ºC and 1 min at 55ºC. All controls (no template controls (NTC) and RT minus controls) were negative. Amplification efficiency (E) was measured by using 10-fold serial dilutions of a positive control PCR template. qRT-PCR efficiency parameters (corroborated in quadruplicate, with intra- and inter-plate replicates) were obtained for each gene (Table S2). Finally, the results were processed by the standard curve method [48].

2.7. Statistical Analysis

The dose-response graphics, its mathematical function and LC_{50} values were calculated using the software package Stratgraphics Centurion 16.0. Data could be adjusted to a dosage-mortality sigmoid curve using the Probit model, and then the LC_{50} was estimated. Gene expression differences (qRT-PCR analysis) were tested for statistical significance by one-way ANOVA followed by a Dunnett´s multiple comparisons test performed with GrapPad Prism 10.1.0 (316). P-value was fixed in ≤ 0.05 for statistically significant values and ≤ 0.01, 0.001 or 0.0001 for high or very high significant values.

3. Results

3.1. Ecotoxicological Parameters

LC_{50} values for both Eu(III) compounds were obtained from dose-mortality curves (Figure S1) of T. thermophila cultures growing in PP210 medium or maintained in 0.01 M Tris-HCl buffer. These values are shown in Table 1. The growth curves and the parameters derived from them are shown in Figure 1. Comparative analysis among the parameters of the growth curves from the strains adapted to Eu(III) compounds with regard to the untreated control shows that the $TtEuCl_3$-adap strain has a growth rate about 3 times lower than the control or the $TtEu_2O_3$-adap strains, and a generation time (Tg) about 3 times longer (Figure 1). In contrast, the $TtEu_2O_3$-adap strain shows a growth rate and Tg very similar to the control strain (Figure 1).

Table 1. LC_{50} (μM) values obtained from the dose-mortality curves shown in Figure S1.

Medium	$EuCl_3$ (μM)	Eu_2O_3 (μM)
Tris-HCl	127.93	173.32
PP210	4830.68	7916.10

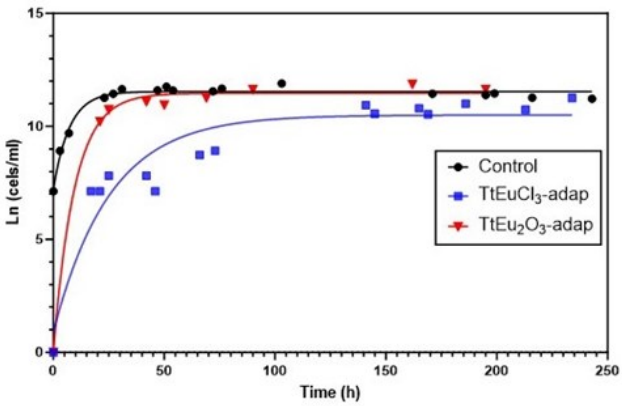

Strain	μ (h^{-1})	Tg (h)	R^2
Control	0.3491	1.98	0.9992
$TtEuCl_3$-adap	0.1134	6.11	0.9996
$TtEu_2O_3$-adap	0.3609	1.92	0.9929

Figure 1. Growth curves of the two adapted strains and the control. Below are the growth parameters: growth rate (μ), generation time (Tg) and correlation coefficient (R^2).

3.2. Oxidative Stress Assessment

The level of oxidative stress was assessed based on the generation of peroxides measured by DCF fluorescence. Figure 2 shows the results expressed as percentage of fluorescent cells (DCF positive) versus two controls (an untreated control and a positive control treated with the oxidizing agent MD). All europium-treated (1 or 24h) and the adapted strains ($TtEuCl_3$-adap and $TtEu_2O_3$-adap) showed significantly lower values ($p \leq 0.001$ or 0.01) than the positive control, and only the $EuCl_3$ 1h sample was significantly lower ($p \leq 0.05$) than the untreated control (Figure 2). All europium-treated or europium-adapted cultures showed similar or lower percentages of fluorescent cells than the untreated control, indicating that Eu(III) does not cause significant levels of oxidative stress (peroxides generation) in this ciliate.

Preprints.org (www.preprints.org) | NOT PEER-REVIEWED | Posted: 19 March 2024 doi:10.20944/preprints202403.1161.v1

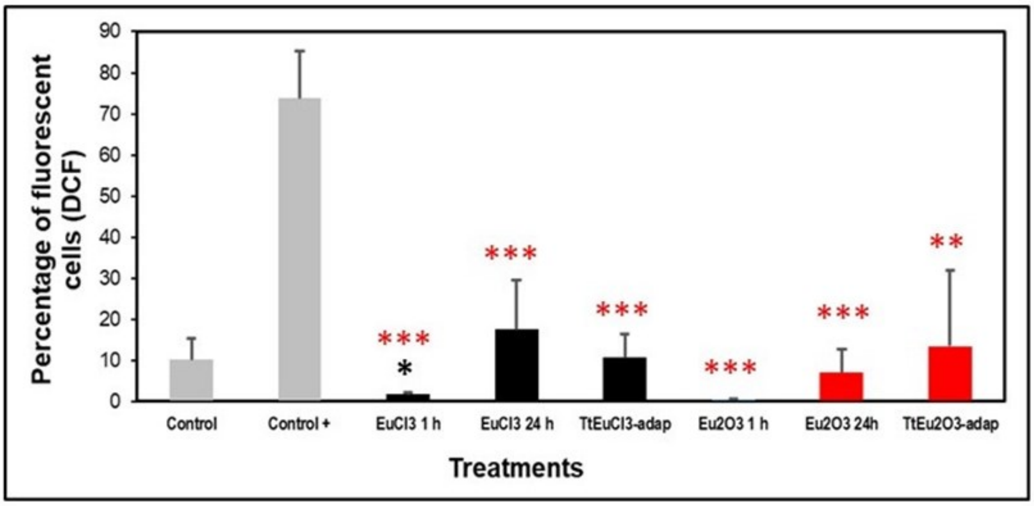

Figure 2. Peroxide generation detected by DCF fluorescence. Gray bars: control (untreated) and positive control (+). Black bars: $EuCl_3$-treated cultures (1 or 24h) and $TtEuCl_3$-adapted strain. Red bars: Eu_2O_3-treated cultures (1 or 24h) and $TtEu_2O_3$-adapted strain. Red stars represent significant differences with respect to the positive control and the black star with respect to the untreated control. Stars denote significant differences [$P \leq 0.05$ (*), $P \leq 0.01$(**), $P \leq 0.001$(***)].

3.3. Comparative Quantitative Expression Analysis of Several Genes Involved in Oxidative and/or General Stress

Thirteen genes involved in general cellular stress or in counteracting oxidative stress, selected based on our previous studies, were chosen for this analysis. These are: one glutathione reductase (*GR1*), two paralogous thioredoxin reductase genes (*TrxR2*, *TrxR5*), the only catalase (*CAT*) and glutathione cysteine ligase (*GCL*) genes present in this ciliate genome, two superoxide dismutases (*Fe-SOD*, *Cu-SOD*), two glutathione S-transferases (*GSTM3*, *GSTZ2*) and the five metallothionein genes (*MTT1*, *MTT2/4*, *MTT3*, *MTT5*) present in this *Tetrahymena* species. qRT-PCR analysis was carried out on cultures of *T. thermophila* treated with $EuCl_3$ (2 mM) or Eu_2O_3 (4 mM) for 24 h, and both adapted strains ($TtEuCl_3$-adap and $TtEu_2O_3$-adap). The *MTT2/4* gene pair has a high identity between them (98%) [49], so it is not possible to design primers that can discriminate between them, and for this reason the obtained gene expression values probably represent the sum of both genes.

Figure 3A shows the results obtained for the five metallothionein isoforms present in this ciliate. The *MTT1* gene is significantly overexpressed under the stress induced by $EuCl_3$ (~ 8-fold) and Eu_2O_3 (~ 51-fold). On the contrary, in both adapted strains this gene is significantly repressed. This MT gene is the most overexpressed under Eu_2O_3 (Figure 3A). The *MTT2/4* pair behaves similarly to *MTT1*, although with much lower induction values under both $EuCl_3$ and Eu_2O_3 treatments. Highlighting the significantly ($p \leq 0.01$) induction (~ 4.8-fold) under Eu_2O_3 stress. The *MTT3* gene, unlike the other MT genes, is most highly overexpressed under the presence of $EuCl_3$ (~ 25-fold) than Eu_2O_3 stress (~ 6-fold), and like the previous ones, it is repressed in both adapted strains (Figure 3A). Finally, the *MTT5* gene is significantly overexpressed (~ 13- fold) almost exclusively under treatment with Eu_2O_3, and unlike the rest of the MT genes, this one shows some significant expression level (~ 2.6-fold) in the Eu_2O_3-adapted strain (Figure 3A).

The two selected *TrxR* genes show very different expression results (Figure 3B), under stress by europium compounds. There is no expression of the *TrxR2* gene under treatment with europium compounds or in both europium-adapted strains. In contrast, *TrxR5* gene expression is induced in cultures treated with $EuCl_3$ (~ 8.5-fold) and strongly and significantly with Eu_2O_3 (~ 39.5-fold) (Figure 3B). Similarly, the expression induction patterns of the two selected *GST* genes are very different (Figure 3C). *GSTM3* gene is induced under stress by $EuCl_3$ (~19-fold) and with Eu_2O_3 (~12.6-fold), both values with very large standard deviations. This could be the reason for not having a significant average value with regard to the control gene. In contrast, the *GSTZ2* gene is only significantly induced (~7-fold) under Eu_2O_3 stress, while in the adapted strains again there is no induction (Figure 3C).

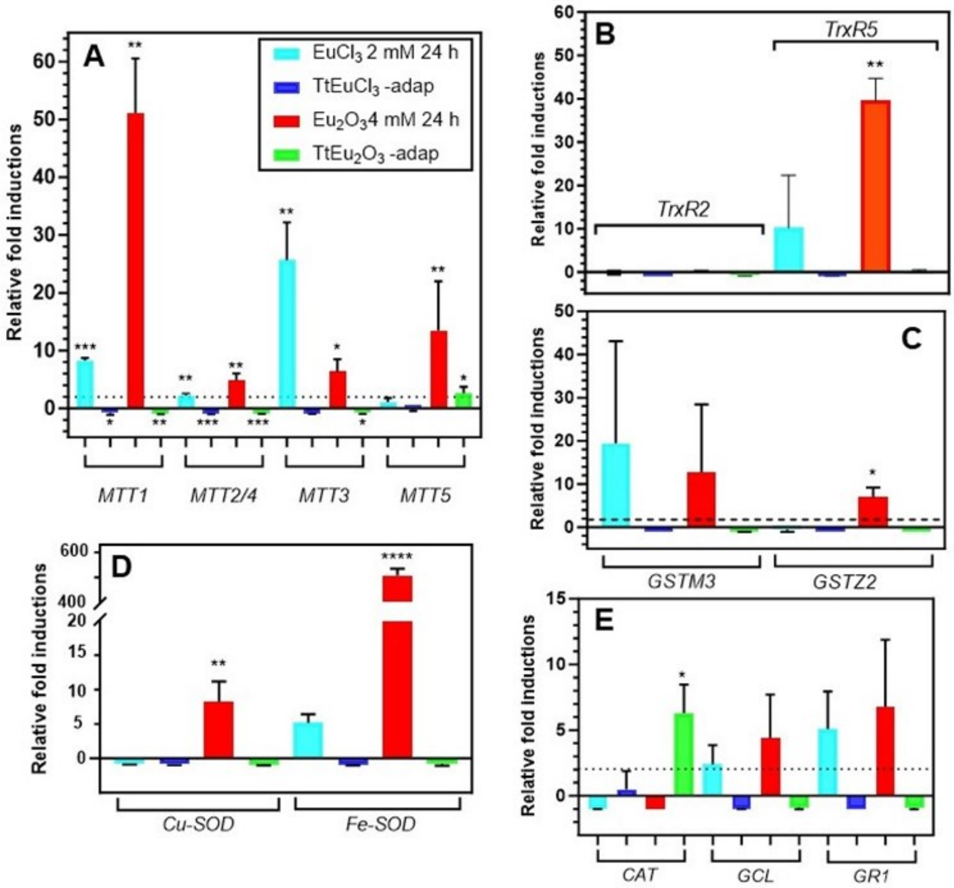

Figure 3. Stress gene expression analysis by qRT-PCR. (A): metalothioneins (*MTT*). (B): thioredoxin reductases (*TrxR*). (C): glutathione S-transferases (*GST*). (D): superoxide dismutases (*SOD*). (E): catalase (*CAT*), glutathione cysteine ligase (*GCL*) and glutathione reductase (*GR*). Stars denote significant differences [$P \leq 0.05$ (*), $P \leq 0.01$(**), $P \leq 0.001$(***), $P \leq 0.0001$ (****)]. A gene expression induction is considered positive when the fold-induction value obtained is > 2 (indicated by the dashed line).

The expression levels of the two *SOD*-encoding genes are shown in Figure 3D. The *Cu-SOD* gene is induced (~ 6.7-fold) exclusively under Eu_2O_3 treatment. However, the *Fe-SOD* gene is induced under treatment with both europium compounds: about 5-fold with $EuCl_3$ and about 500-fold with Eu_2O_3, this average value being highly significant ($p \leq 0.0001$) with respect to the control gene. In both adapted strains, no expression of these genes is detected, but rather some repression (Figure 3D).

The expression results of the last three selected genes (*CAT*, *GCL* and *GR1*) are shown in Figure 3E. The catalase (*CAT*) gene is repressed in the $EuCl_3$- and Eu_2O_3-treated cultures, but some significant induction (~ 6-fold) arises in the $TtEu_2O_3$-adap strain. The other two genes (*GCL* and *GR1*) show a very similar gene expression induction pattern, with expression only under $EuCl_3$ and Eu_2O_3 treatments, but with average values with high standard deviations. The two adapted strains show no expression of these two genes, but there is some repression. (Figure 3E).

Preprints.org (www.preprints.org) | NOT PEER-REVIEWED | Posted: 19 March 2024 doi:10.20944/preprints202403.1161.v1

3.4. Ultrastructural Analysis

The ultrastructural analysis was performed on cultures treated (1 or 24h) with $EuCl_3$, the two types of adapted strains (Tt$EuCl_3$-adap and TtEu_2O_3-adap) and a control culture (without any treatment). The analysis of cultures treated with Eu_2O_3 was discarded because of its low toxicity. Figures 4B, 4C and 4D show different cytoplasmic regions (macronucleus, vacuole, mitochondria) and an image of a *T. thermophila* whole cell (Figure 4A) as a control. Cells from a culture grown in PP210 and treated with $EuCl_3$ (2 mM) for 1h are shown in Figure 5. The macronucleus (Ma) is structurally similar to that shown by control cells, but with a larger number of nucleolar bodies (region within the ellipse) at its periphery (Figure 5A).

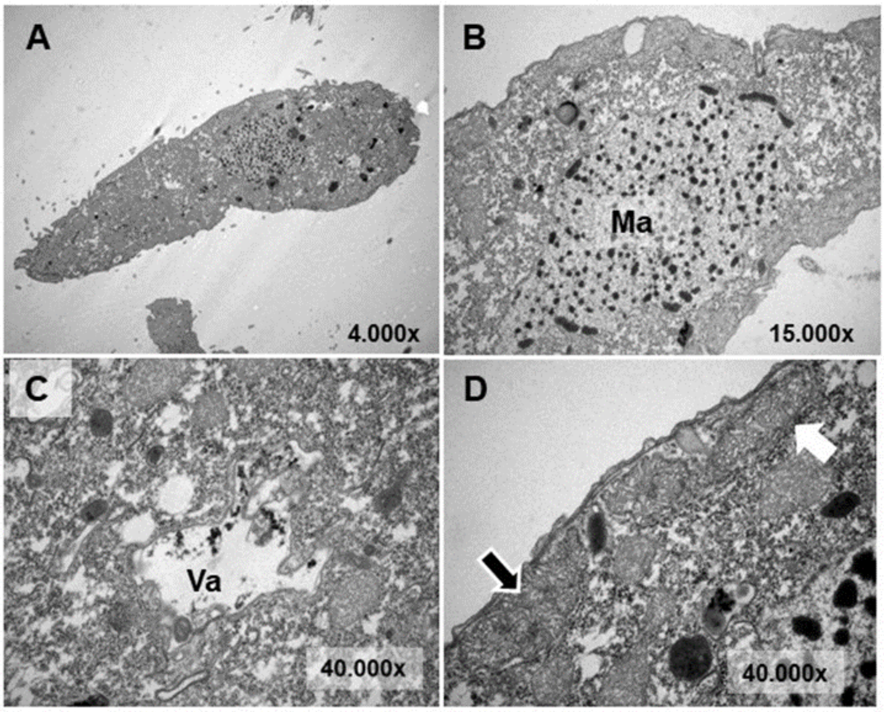

Figure 4. TEM images of cells from a control culture (untreated). (A): *T. thermophila* whole cell. (B): Macronucleus (Ma). (C): Vacuole (Va). (D): Mitochondria (arrows).

A greater number of vacuoles with an electrodense granular content are visible (arrows in Figures 5A,B). These vacuoles (~2-3 µm in length) bioaccumulate an electrodense granular material, presumably europium (Figures 5C–E). The vacuolar membrane enclosing this electrodense granular material is well seen in Figure 5D (arrow). Eventually, this granular content is expelled out of the cell by fusion of the vacuolar membrane with the ciliate envelope (Figure 5F). In the culture treated for 24h with $EuCl_3$, a higher number of vacuoles at different bioaccumulation stages of the electrodense granular material is observed (Figure 6A,B). The electrodense granules (~0.1 µm in diameter) condense into larger granules or clusters within the vacuole (Figure 6C,D).

Preprints.org (www.preprints.org) | NOT PEER-REVIEWED | Posted: 19 March 2024 doi:10.20944/preprints202403.1161.v1

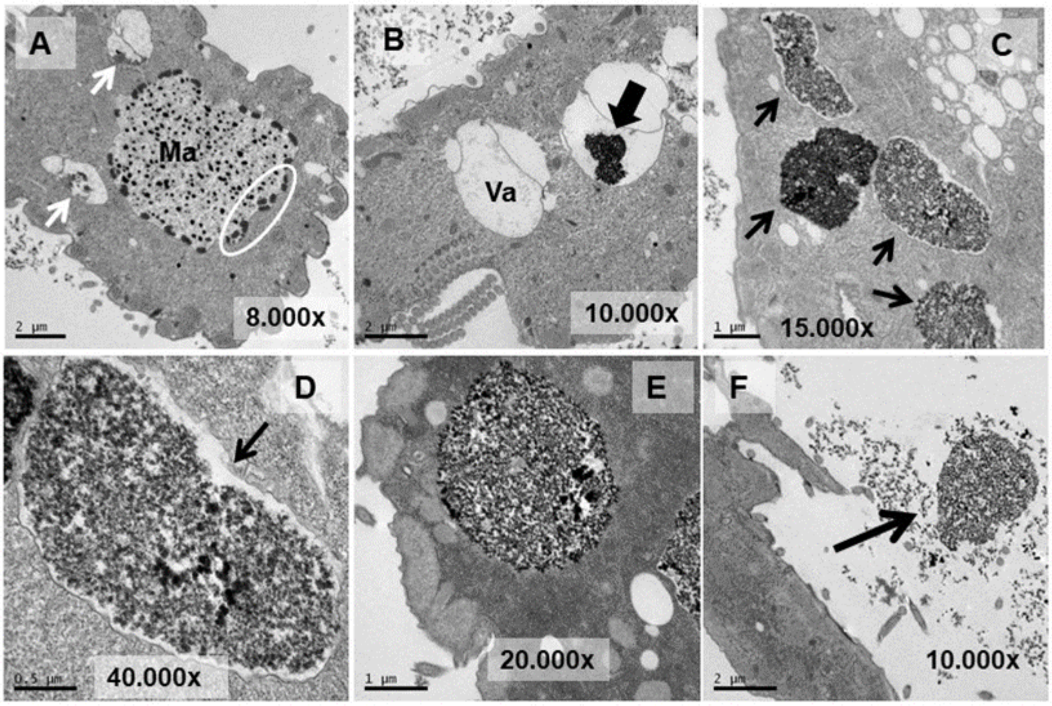

Figure 5. TEM images of cells treated with $EuCl_3$ (2 mM, 1h treatment). (A): Macronucleus (Ma) with a large number of nucleolar bodies (region within the ellipse). Vacuoles with an electrodense content (arrows). (B): Vacuole (Va). Black arrow indicates electrodense content. (C): Numerous vacuoles (arrows) containing an electrodense granular material (bioaccumulation). (D and E): Magnified images of vacuoles containing electrodense material. In (D) the vacuolar membrane is observed (arrow). (F): Ejection of the electrodense granular content (arrow) outside the cell.

In the Tt$EuCl_3$-adap strain, the electrodense granular content is more condensed within the vacuole and surrounded by a wide electrolucent region (Figure 7A,B,D). Membrane structures sometimes appear in this region surrounding the electrodense granular material (arrows in Figure 7E,F). In Figure 7A (dashed line box) a large number of lipid drops are detected that both fuse with each other and with the vacuoles containing the electrodense granular material (arrows in Figure 7A,B). Upon fusion of the lipid drop membrane with that of the vacuole, it deposits its contents inside the vacuole and surrounding the granular material. When the granular contents of these vacuoles are excreted, they are also accompanied by the electrolucent enveloping region (arrows in Figure 7C). The contents of some vacuoles also present electrodense fibrillar structures, in addition to the granular material, which are also expelled outside the cell (arrows in Figure 7C,G).

Preprints.org (www.preprints.org) | NOT PEER-REVIEWED | Posted: 19 March 2024 doi:10.20944/preprints202403.1161.v1

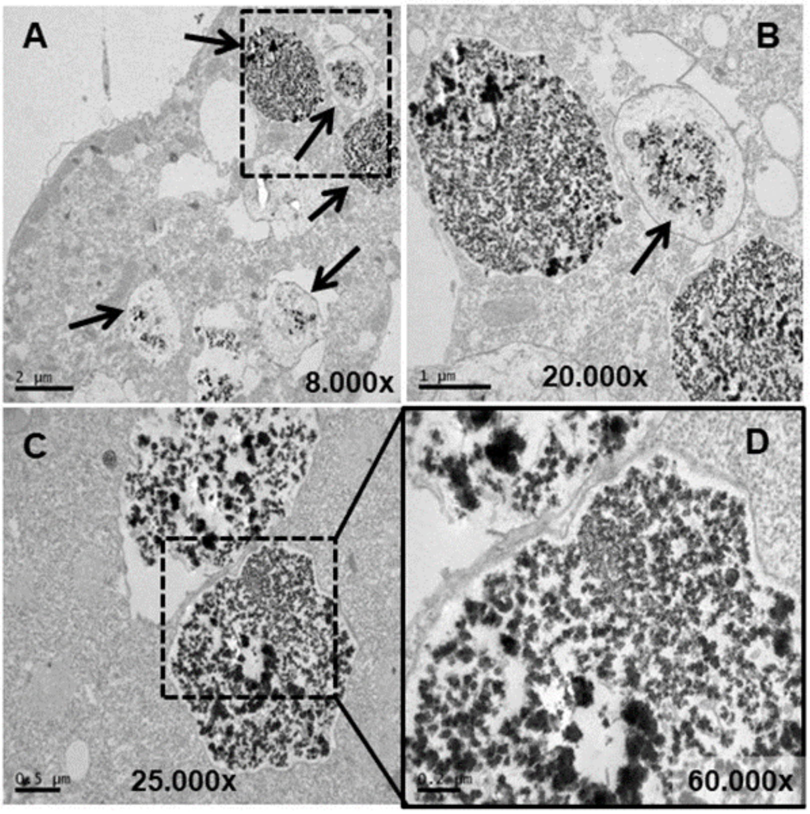

Figure 6. TEM images of cells treated with $EuCl_3$ (2 mM, 24h treatment). (A): Vacuoles with different levels of electrodense granular material bioaccumulation (arrows). (B): Magnification of the region (delimited by the square with the dashed line) in panel A. (C): Vacuoles with granular electrodense material. (D): Magnification of the region (delimited by the square with the dashed line) in panel C. **.**

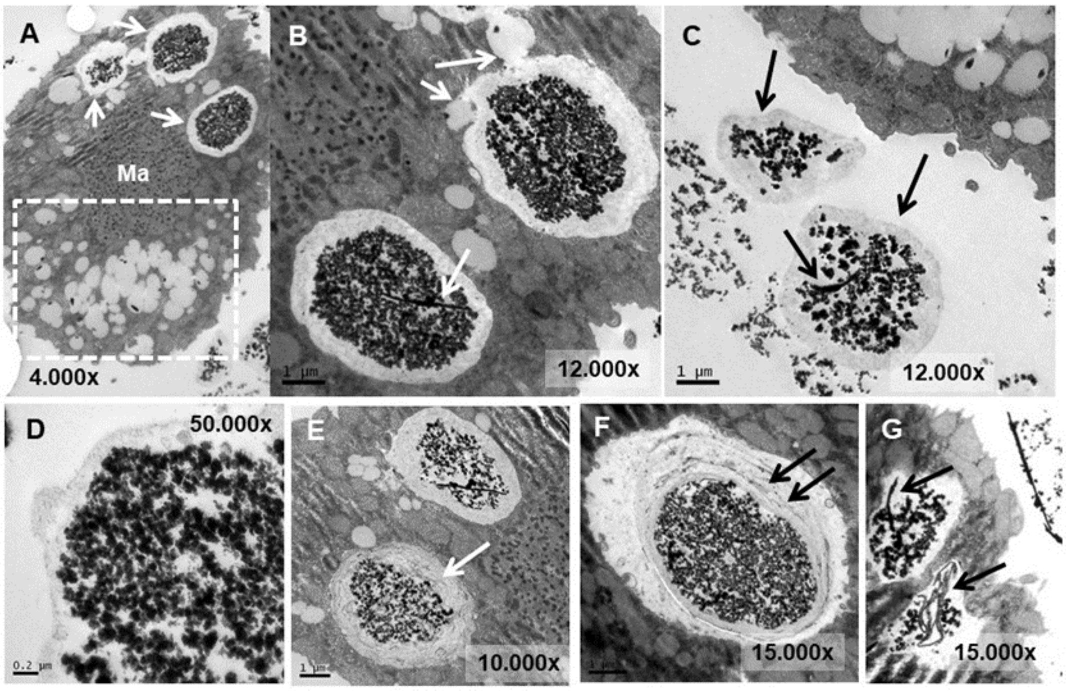

Figure 7. TEM images of TtEuCl_3-adap cells. (A): Vacuoles with electrodense condensed granular content and surrounded by an electrolucent material originating from fusion with numerous lipid

droplets (arrows). Region with numerous lipid droplets (dashed line box). Ma (macronucleus). (B): Magnified region from panel A. (C): The granular contents from vacuoles with their peripheral electrolucid region are excreted out of the cell. (D): Magnified detail of one of the excreted materials. (E and F): The electrolucent material sometimes contains membranous or fibrillar elements surrounding the electrodense granular content (arrows). (G): In some vacuoles, an electrodense fibrillar content is observed together with the granular one.

In the strain adapted to high concentrations of Eu_2O_3 (TtEu_2O_3-adap) the vacuoles containing the electrodense granular material are similar to those of the strain adapted to $EuCl_3$ (Tt$EuCl_3$-adap), but the electrolucent envelope, deposited between the vacuolar membrane and the granular material, is thinner (Figure 8A,B). Likewise, a large number of lipid drops (dashed line box in Figure 8C) and numerous autophagosomes are detected in these cells. (Figure 8B,D). The electrodense granular content is expelled from the cell maintaining the shape it had inside the vacuole (Figure 8C), together with bundles of an electrodense fibrillar material (Figure 8E).

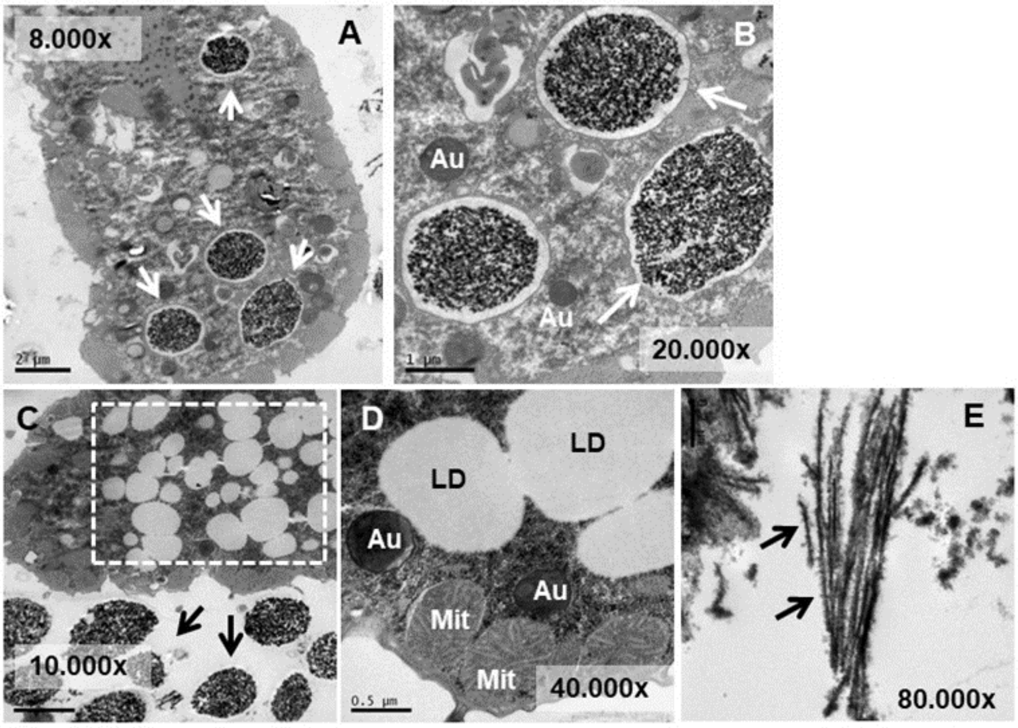

Figure 8. TEM images of TtEu_2O_3-adap cells. (A): Vacuoles with electrodense granular contents and a thin electrolucid envelope (arrows). (B): Magnified region from panel A. Au (autophagosomes). (C): Region with numerous lipid droplets (dashed line box). Electrodense granular material ejected out of the cell (arrows). (D): Cytoplasmic region with mitochondria (Mit), autophagosomes (Au) and lipid droplets (LD). (E): Bundles of fibers with adhered electrodense material ejected out of the cell (arrows). .

3.5. Microanalysis (TEM-XEDS)

To corroborate the presence of europium, the Tt$EuCl_3$-adap strain was chosen to analyze the elemental composition of the electrodense vacuolar deposits by TEM-XEDS. Figure 9 shows the spectrum obtained by TEM-XEDS from a semi-thin section of cells from the Tt$EuCl_3$-adap strain. An electron micrograph from which the microanalysis was performed is shown in Figure 9. The spectrum shows the characteristic peaks of europium (red arrows), as well as chlorine, carbon and oxygen. The presence of copper is due to the nature of the grid used. Phosphorus (white arrow) is also detected in the spectrum (Figure 9).

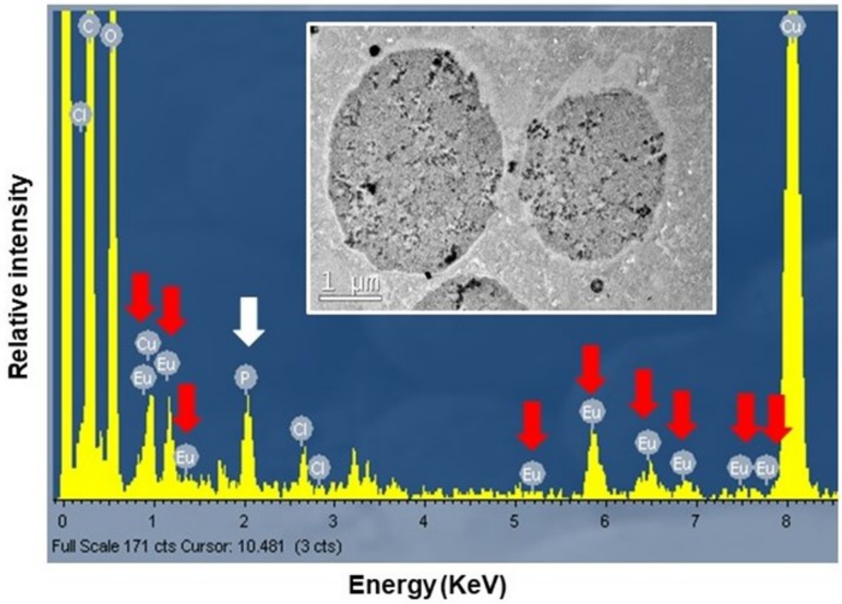

Figure 9. Spectra obtained by TEM-XEDS analysis. Internal TEM micrograph shows vacuoles on which elemental microanalysis was performed. Red arrows indicate the presence of europium, and the white arrow shows the presence of phosphorus.

4. Discussion

As described in the introduction, europium compounds are of great interest in biology, medicine and various technologies related to imaging and optics. However, little is known about their potential toxicity in eukaryotic cells, and possible cellular strategies to counteract their toxicities such as bioaccumulation and/or biomineralization, among others.

4.1. Toxicological and Growth Kinetics Parameters

As is the case of other metal(loid)s **[50,51]**, the presence of organic matter in the medium significantly increases the value of the LC_{50} parameter with respect to that obtained in an inorganic medium (buffer), and this is due to the metal(loid)s chelating capacity of the organic matter [36]. Therefore, a higher amount of metal(loid) is required to obtain 50% cell mortality (LC_{50} value). The same is true for both europium compounds: in the PP210 growth medium with $EuCl_3$ the LC_{50} value is increased by about 37-fold with respect to the value obtained in Tris-HCl, while with Eu_2O_3 this increase is about 45-fold. From the LC_{50} values it can be inferred that $EuCl_3$ is more toxic (1.3 - 1.6-fold) than Eu_2O_3, which could be due to the higher solubility of $EuCl_3$ in an aqueous medium, thus making Eu(III) more toxic.

The maximum concentration (5.5 mM) of $EuCl_3$ used in the Tt$EuCl_3$-adap strain represents ~1.14-fold of the LC_{50} value of the wild-type (non-adapted) strain in PP210 or ~43-fold in Tris-HCl. Whereas in the TtEu_2O_3-adap strain, the maximum concentration achieved (8.5 mM Eu_2O_3) represents ~1.07-fold of the LC_{50} of the wild-type strain in PP210 or ~49-fold in Tris-HCl.

In the ciliate Paramecium bursaria [31], a mortality close to 80% is obtained with 0.1 mM Eu(III), a concentration much lower than the LC_{50} value obtained in *T. thermophila* for both europium compounds. This may be due to several factors, such as the europium compound used (europium acetate hydrate), the medium where the treatment was performed, the cell concentration used and/or the type of ciliate.

The Eu(III) toxicity parameters used for other eukaryotic microorganisms are different. A 20% growth inhibition (IC_{20}) of a yeast *Saccharomyces cerevisiae* cell population is achieved with $EuCl_3$ 0.131 mM [52]. In the marine microalga *Skeletonema costatum* [53], 50% population growth inhibition or half-effective concentration (EC_{50}) treated with europium nitrate is obtained at 29.16 µM. Regardless of

Preprints.org (www.preprints.org) | NOT PEER-REVIEWED | Posted: 19 March 2024 doi:10.20944/preprints202403.1161.v1

the impossibility to compare toxicity values between different microorganisms, by using very different parameters and conditions, we can infer that *T. thermophila* seems to be more resistant to europium compounds than shown by other eukaryotic microorganisms.

Biotoxicity tests performed in distilled water on *T. thermophila* [54] using other lanthanides than Eu(III), such as La(III), Ce(III), Pr(III), Nd(III) or Gd(III), both in the form of oxides or nitrates, showed EC_{50} (24h) values > 100 mg/L for rare earth oxides, and EC_{50} (24h) values = 28-42 mg/L for nitrates. The authors consider that these Ln concentrations are not sufficiently toxic for this ciliate. In a different species, *T. shanghaiensis* [55], also using other Ln than Eu(III), the IC_{50} values (24h and in rich growth medium) were between 0.34 mM (Gd) and 2 mM (La).

The growth curve parameters of the two strains adapted to increasing concentrations of europium compounds show that the TtEuCl$_3$-adap strain decreases its growth rate by about 3-fold with respect to both the control strain and the TtEu$_2$O$_3$-adap strain (which has very similar growth parameters to the control), and the Tg increases by a factor of three. Consequently, this TtEuCl$_3$-adap strain grows about 3-fold slower than the control and the TtEu$_2$O$_3$-adap strain. This effect of decreased growth rate linked to metal adaptation has also been detected in other strains of this same ciliate adapted to Cd, Pb or Cu (unpublished data from our research group).

In the thermophilic bacterium *Thermus scotoductus* [24] exposure at $EuCl_3$, low concentrations (0.01 - 0.5 mM) increases the maximum growth rate relative to the control, whereas at higher concentrations (1 mM) it decreases the growth rate. In contrast, in a *Clostridium* sp. strain [56], a decrease in growth rate is observed from a $EuCl_3$ concentration as low as 0.01 mM, and the decrease is greater as the concentration increases. Therefore, under similar conditions the effect of the same Eu(III) compound can be very different depending on the microbial type.

4.2. Oxidative Stress Assessment

None of the treatments performed with both Eu(III) compounds showed a significant increase over the untreated control. Therefore, we cannot consider that Eu(III) induces peroxide or hydroxyl radicals generation in *T. thermophila*, which does not imply that other types of radicals that induce oxidative stress can be originated. However, in this same ciliate, exposure to oxides of various lanthanides, other than Eu(III), induced oxidative stress (hydroxyl radicals) [54]. The main difference between these experiments and our results with Eu(III) is that they were performed in distilled water and not in growth medium, regardless of the lanthanides used.

A possible reason for the non-detection of peroxide or hydroxyl radicals could be due to the protective system developed by the ciliate using antioxidant enzymes (like catalase, glutathione peroxidase, peroxiredoxin reductase, thioredoxin reductase, etc.) to minimize the lethal effects of oxidative stress caused by Eu(III).

Both $Eu(OH)_3$ nano-bars and spheres as well as $Eu(NO_3)_3$ induce angiogenesis (formation of new blood vessels, during embryonic development, growth and/or tumorization) in zebrafish embryos [57]. This induction of the angiogenic process is related to the production of H_2O_2 by these Eu compounds, i.e.; Eu(III) → ROS (reactive oxygen species) → angiogenesis. In natural processes (embryogenesis), ROS production modulates angiogenesis through a reversible oxidase [57]. There is, therefore, some connection between Eu(III) and the direct or indirect production of peroxides.

4.3. Expression Analysis of Genes Involved in General and/or Oxidative Stress Cell Response

For most of the genes analyzed, $EuCl_3$ (2 mM, 24h) and Eu_2O_3 (4 mM, 24h) treatments are the ones that trigger their (sometimes-significant) over-expression. In strains adapted to Eu(III) compounds, only strain TtEu$_2$O$_3$-adap shows significant ($p \leq 0.05$) over-expression of the catalase-encoding gene (Figure 3E). This could corroborate the formation of a certain amount of peroxide radicals in this adapted strain, that catalase would degrade into water and oxygen. Although the DCF fluorescence results are not significant with respect to the control, but a wide standard deviation (SD) is observed, and according to the Brown-Forsythe test [58], it is significantly different at $p < 0.05$ (Figure 2). The adaptation of these strains means that many of the genes linked to oxidative stress

Preprints.org (www.preprints.org) | NOT PEER-REVIEWED | Posted: 19 March 2024 doi:10.20944/preprints202403.1161.v1

and those encoding metallothioneins, with the exception of catalase in the Eu_2O_3-adapted strain, do not need to be overexpressed.

The reduction of H_2O_2 to H_2O involves the enzyme glutathione peroxidase and the reducing power is acquired from peroxiredoxins, and these acquire the reducing power from reduced thioredoxins, so thioredoxin reductases are important in this process. In *T. thermophila* genome there are five thioredoxin reductase paralogous genes (*TrxR1*-*TrxR5*), of which three of them are selenoproteins and two (*TrxR2* and *TrxR5*) are not. We have chosen the latter two TrxRs isoforms because of their high over-expression with arsenic (arsenate) [42], which is a metalloid that cause elevated oxidative stress. Results show that only the *TrxR5* isoform responds to both Eu(III) compounds, the over-expression obtained in the culture treated with Eu_2O_3 being significant ($p \leq 0.01$). This same *TrxR5* gene from *T. thermophila* is over-expressed under treatment with the herbicide Paraquat that causes oxidative stress [34].

The overexpression (although not significant, probably due to the large values of their SDs) of the genes *GCL* (involved in glutathione (GSH) biosynthesis) and *GR1* (converts GSSG to GSH) could indicate the GSH requirement for glutathione peroxidases (GPx) that also reduce H_2O2 induced by Eu(III) treatments. Likewise, GSH is the substrate transferred by GSTs to potentially toxic molecules blocking their toxicity. Among the 70 GST paralogous genes existing in the *T. thermophila* genome [59], only two (*GSTM3* and *GSTZ2*) have been selected for this study. A significant ($p \leq 0.05$) over-expression of *GSTZ2* is obtained in the culture treated (24h) with Eu_2O_3, and although there is also an induction of *GSTM3* gene expression in both Eu(III) treated cultures, these are not statistically significant (probably due to their large SDs). The *GSTZ2* gene is also over-expressed in *T. thermophila* with both selenite and selenate treatments, which cause elevated oxidative stress [37].

Both superoxide dismutase genes (*Cu-SOD* and *Fe-SOD*) are significantly induced against europium oxide (Figure 3D), especially *Fe-SOD* up to about 500-fold ($p \leq 0.0001$). These enzymes convert the superoxide ion (highly toxic) into H_2O_2, which is then inactivated by catalase. Overexpression of both *SODs* would mean that superoxide ion originates under europium oxide stress. Although both enzymes can localize to the cytosol, Fe-SOD could also be in the mitochondria [60], so the dramatic overexpression (Figure 3D) of this enzyme could likewise mean dysfunction in ciliate mitochondria. Another possible interpretation of the high increase of the gene expression encoding Fe-SOD could be that SODs are ideal ligands for Eu(III) ions, as evidenced by the spectrofluorometric determination of these enzymes using an Eu-tetracycline probe [61]. If this interaction occurs *in vivo* it would block the enzyme, so that the cell would have to synthesize much more of it. In diverse plants, other lanthanides (La, Ce) induce intracellular increases in SOD, CAT, GSH and the formation of hydroxyl ions, H_2O_2, superoxide ions and lipid peroxidation [2].

The ranking of the average relative induction values for $EuCl_3$ (24h) treatment is *GSTM3* > *TrxR5* > *Fe-SOD* ≈ *GR1* > *GCL*, and for Eu_2O_3 (24h) stress is *Fe-SOD* >> *TrxR5* > *GSTM3* > *GSTZ2* ≈ *Cu-SOD* ≈ *GR1* > *GCL*. The first three antioxidant genes in both rankings coincide although in different order and with very different induction values, and likewise the last two in the rankings (genes involved in glutathione metabolism). Although it is the same cation Eu(III), it is forming different compounds; one ($EuCl_3$) with higher solubility and the other (Eu_2O_3) with nanoparticulated nature (45-58 nm) and less water-soluble. These physical differences, as well as the ROS type produced by the Eu(III) cation, could explain these differences in both gene expression induction rankings.

Both europium compounds induce the expression of all *T. thermophila* MT genes, at different levels, except *MTT5*, which is only significantly induced ($p \leq 0.01$) under europium oxide stress. In addition, the TtEu$_2$O$_3$-adap strain shows a significant ($p \leq 0.05$) overexpression (2.6-fold) of the *MTT5* gene bordering the threshold minimum fold-change value (2-fold, dashed line in Figure 3A), that by consensus is considered as a significant relative quantification of the gene expression induction. Under $EuCl_3$ stress (24h), the ranking of *MTT* gene expression induction values is *MTT3* > *MTT1* > *MTT2/4*. However, this ranking under Eu_2O_3 stress (24h) is *MTT1* >> *MTT5* > *MTT3* > *MTT2/4*. As found in previous work **[62,63]**, the ranking of these MT genes varies depending on the metal and treatment conditions. In this case, it is the same metal (Eu), although forming part of a different compound.

In the study of the induction of *T. thermophila* metallothionein genes by metal(loid)s, it is common to use divalent cations [62], but it is more unusual to find studies with trivalent cations. Treatment (24h) with arsenite [As(III)] induces overexpression of *MTT5* and *MTT1* genes (*MTT5* > *MTT1*) [42], and lanthanum [La(III)] induces expression of *MTT1* and *MTT2* genes [64]. In this latter study, fluorescence analysis indicates that La(III) binds to both metallothioneins via the oxygen atoms of aspartic or glutamic acid residues. A fluorimetric method of quantifying MTs is based on the use of lomefloxacin-europium(III) complex as a fluorescent probe, since MT reacts with the LMLX-Eu(III) system forming a stable ternary complex (LMLX-Eu(III)-MT) [65]. Therefore, in the case of both La(III) and Eu(III) it is shown that these trivalent cations can interact with these metal chelating proteins. Furthermore, a toxigenomic analysis [52] using $EuCl_3$ suggests that Eu(III) can disrupt the function of chaperones and cochaperones that present metal binding sites, thus promoting toxicity in yeast. This could equally explain the overexpression of the *MTT3* gene by $EuCl_3$ treatment, which is one of the genes, together with *MTT1*, whose basal constitutive expression is highest, and is considered to play a role in the intracellular homeostasis of essential metals such as Zn(II) or Cu(II) [63]. Being possibly disrupted by Eu(III), the cell requires more of it for its viability. Lanthanides react with biologically active compounds replacing Ca(II) ions among others, such as Zn(II), Mg(II), Fe(II) [66]. If in MTT3 Zn(II) is replaced by Eu(III) blocking the function of this MT, the cell would need synthesize more of this protein, hence the increased overexpression of this *MTT3* gene.

4.4. Ultrastructural Modifications and Microanalysis

Ultrastructural analysis from the culture treated with $EuCl_3$ (1h) reveals an increase of the number of nucleolar bodies in the macronucleus of *T. thermophila*. It is known that nucleoli undergo structural changes as a cellular response to many environmental stressors (known as "nucleolar stress"), so being a bioindicator of the cell stress [67]. An increase in the number of nucleoli could mean a greater need for ribosome biosynthesis to keep the cell growing despite the toxic effect of europium on cell growth (as in the $TtEuCl_3$-adap strain, where its growth rate decreases by about 3-fold compared to the control). The increase in the number and size of nucleoli has been used as an indicator of cancerous lesions in many types of tumors, and this increase is attributed to the need for protein biosynthesis in cancer cells **[68,69]**. Likewise, in hypertrophied human hearts (with hyperfunction) the number of nucleoli is increased, indicating an increase in RNA synthesis [70].

Another characteristic of these cells is an increase in the number of vacuoles with a granular electrodense content. This material (europium) is eventually expelled out of the cell. In longer treatments (24h) with $EuCl_3$, the number of vacuoles increases, and different bioaccumulation phases of this material inside the vacuoles are observed. In the literature on lanthanide bioaccumulation (including europium), the most quantitatively relevant is that carried out by microorganisms (non-photosynthetic) and phytoplankton (including microalgae) [1]. Other authors [71] also highlight the Ln-bioaccumulation by zooplankton, being an excellent bioindicator of their bioavailability in freshwater ecosystems. This process of Eu(III) bioaccumulation probably complexed with biomolecules, and subsequent elimination outside the cell, constitutes a detoxification mechanism (widespread among eukaryotes) that involves an increase in vacuolar activity.

The main structural difference between the vacuoles with the electrodense granular content from the $EuCL_3$-treated culture and the $TtEuCl_3$-adap or $TtEu_2O_3$-adap strains is the thick electrolucid region surrounding the bioaccumulated material. This electrolucid region is formed by fusion of the vacuolar membrane with numerous lipid droplets. Some of these regions contain membranous debris to which europium can bind and form electrodense fibrillar structures.

Lipid droplets can be a biomarker, a vehicle and a facilitator for cellular stress response and survival [72]. Lipid droplets as potential sources of nutrients and energy respond to starvation stress [72], are connected to autophagy [73], involved in cross organelle communication [74] and infectious diseases by viruses, bacteria or protozoa [75]. Indeed, in the $TtEu_2O_3$-adap strain together with large lipid droplets, numerous autophagosomes are detected (Figure 8D), indicating that both processes are connected to stress originating from europium oxide nanoparticles. Likewise, an increase in lipid droplets has been observed in diverse eukaryotic cells under metal(loid) stress, such as Cd(II)

 doi:10.20944/preprints202403.1161.v1

[76] or Cu(II) [77], and in *T. thermophila* under metal nanoparticles stress (copper oxide nanotubes) [78] or As(III) treatment [42].

When pathogenic microorganisms infect a eukaryotic cell, for example: *Chlamydia* bacteria or the protozoan parasite *Toxoplasma*, appears to accumulate lipids by trafficking lipid droplets from the host cell to the vacuoles where the pathogen replicates [72]. It is possible that a similar mechanism of isolation of toxic particulate elements (such as europium nanoparticle aggregates) could occur in *T. thermophila* cells under the extreme stress that strains adapted to high concentrations of Eu(III) compounds undergo. Once the toxic element is isolated in a vacuole with membrane remnants and high lipid content, it would be expelled outside the cell.

TEM-XEDS microanalysis of the electrodense granular content of the vacuoles of the TtEuCl_3-adap strain has shown a spectrum with the 8-9 peaks or regions where Eu(III) is detected, very similar to that shown by other authors [24]. Which corroborates that the vacuolar content in these cells contains europium. Moreover, in the same spectrum a significant peak identified as phosphorus appears. The soluble Eu(III) could react with cytoplasmic phosphates or polyphosphates to form europium phosphate ($EuPO_4$).

Both intracellular and extracellular (biosorption) nano-biomineralization and bioaccumulation of lanthanides (including europium) have been described in both bacteria **[24,79]** and eukaryotic microorganisms (yeast and microalgae) **[79,80]**. The thermophilic bacterium *T. scotoductus* [24] can bioaccumulate intra- and extracellularly Eu(III) biomineralized as $Eu_2(CO_3)_3$ (europium carbonate). Likewise, Eu(III) intracellular bioaccumulation could be facilitated by polyphosphate metabolism. In fact, both electron microscopy and microanalysis have shown intracytoplasmic electrodense granules composed of Eu(III) and phosphate [24]. Lanthanide phosphates and carbonates are insoluble under physiological conditions and precipitate. Both *in vivo* and *in vitro*, using the microalga *Chlorella vulgaris* [80], Eu(III) chloride binds preferentially to phosphate groups.

Several studies have reported phosphate mineralization of both light (Ce) and heavy (Yb) lanthanides in the yeast *S. cerevisiae*. Needle-shaped Ce(III) phosphate nanocrystals were detected in *S. cerevisiae* cells after exposing the cells to a Ce(III) solution [81]. Similarly, in this same yeast, the formation of ytterbium (Yb) phosphate nano-particles on the cell surface as a precipitate after an adsorption process has been described [82]. In a strain of *T. thermophila* adapted to high amounts of Pb(II), a process of biomineralization of this metal to chloropyromorphite ($Pb_5[PO_4]_3Cl$) has been studied based on the utilization of intracellular phosphate [83]. Therefore, it is not surprising that, like in other microorganisms, phosphate is used to carry out a detoxification process.

5. Conclusions

- In *T. thermophila*, $EuCl_3$ is more toxic than Eu_2O_3. Regardless of it, this microorganism seems to be more resistant to europium compounds than shown by other reported eukaryotic microorganisms.
- Cell adaptation to $EuCl_3$ affects the growth rate of the adapted strain, but does not affect the growth of the Eu_2O_3-adapted strain.
- The absence of peroxides or hydroxyl radicals after treatment with both Eu(III) compounds could be due to the protection system developed by the ciliate with the intracellular increase of antioxidant enzymes, as confirmed, partially, by the overexpression of the genes encoding them.
- The overexpression of metallothioneins under treatment with Eu(III) compounds supports the possibility that this lanthanide may interact with the -SH groups of the cysteine residues from MTs and/or displace essential cations of these proteins during their homeostasis function.
- Both lipid metabolism and autophagy are involved in the cellular response to europium stress.
- Like other microorganisms, in *T. thermophila* the main detoxification mechanism of Eu(III) compounds is bioaccumulation into vacuoles and subsequent expulsion out of the cell, probably linked to a biomineralization process to europium phosphate.

Supplementary Materials: The following supporting information can be downloaded at the website of this paper posted on Preprints.org., Figure S1: Dose-mortality curves. (A): $EuCl_3$ treatments. (B): Eu_2O_3 treatments. Histograms: (A1, A3, B1 and B3). Adjusted model with 95% confidence intervals: (A2, A4, B2 and B4); Table S1: Sequences and features of the primers used in the qRT-PCR analysis; Table S2: Quantitative RT-PCR standard-curve parameters.

Author Contributions: Conceptualization, J.C.G and A.M.G.; investigation, P.A., J.B., F.A. P.dF. and A.M.G.; writing—original draft preparation, J.C.G. and A.M.G.; writing—review and editing, J.C.G.; supervision, J.C.G. and A.M.G.; funding acquisition, J.C.G. All authors have read and agreed to the published version of the manuscript.

Funding: The Spanish Ministry of Economy and Competitiveness, grant number CGL2016-75494-R awarded to J.C.G., funded this research.

Institutional Review Board Statement: Not applicable.

Informed Consent Statement: Not applicable.

Data Availability Statement: Data will be made available on request.

Conflicts of Interest: The authors declare no conflicts of interest.

References

1. Blinova, I.; Muna, M.; Heinlaan, M.; Lukjanova, A.; Kahru, A. Potential hazard of lanthanides and lanthanide-based nanoparticles to aquatic ecosystems: data gaps, challenges and future research needs derived from bibliometric analysis. Nanomaterials. **2020**, 10, 328. https://doi:10.3390/nano10020328.
2. Gonzalez, V.; Vignati, D.A.L.; Leyval, C.; Giamberini, L.; Environmental fate and ecotoxicology of lanthanides: are they a uniform group beyond chemistry? Environ. Int. **2014**, 71, 148-157. https://dx.doi.org/10.1016/j.envint.2014.06.019.
3. Gonzalez, V.; Vignati, D.A.L.; Pons, M-N.; Montarges-Pelletier, E.; Bojic, C.; Giamberini, L. Lanthanide ecotoxicity: first attempt to measure environmental risk for aquatic organisms. Environ. Pollut. **2015**, 199, 139-147. https://dx.doi.org/10.1016/j.envpol.2015.01.020.
4. Martino, C.; Chianese, T.; Chiarelli, R.; Roccheri, M.C.; Scudiero, R. Toxicological impact of rare earth elements (REEs) on the reproduction and development of aquatic organisms using sea urchins as biological models. Int. J. Mol. Sci. **2022**, 23, 2876. https://doi.org/10.3390/ijms23052876.
5. Pagano, G.; Thomas, P.J.; Nunzio, A.D.; Trifuoggi, M. Human exposures to rare earth elements: present knowledge and research prospects. Environ. Res. **2019**, 171, 493-500. https://doi.org/10.1016/j.envres.2019.02.004.
6. Balaram, V. Rare earth elements: A review of applications, occurrence, exploration, analysis, recycling, and environmental impact. Geosci. Front. **2019**, 10, 1285-1303. https://doi.org/10.1016/j.gsf.201812.005.
7. Cotruvo, Jr. J.A. The chemistry of lanthanides in biology: recent discoveries, emerging principles, and technological applications. ACS. Cent. Sci. **2019**, 5, 1496-1506. https://doi.101021/acscentsci.9b00642.
8. Bünzli, J-C.G. Lanthanide light for biology and medical diagnosis. J. Lumin. **2016**, 170, 866-878. http://dx.doi.org/10.1016/j.jlumin.2015.07.033.
9. Qin, X.; Wang, J.; Yuan, Q.; Synthesis and biomedical applications of lanthanides-doped persistent luminescence phosphors with NIR emissions. Front. Chem. 2020, 8: 608578. https://doi.org/10.3389/fchem.2020.608578
10. Syamchand, S.S.; Sony, G. Europium enabled luminescent nanoparticles for biomedical applications. J. Lumin. **2015**, 165, 190-215. http://dx.doi.org/10.1016/j.jlumin.2015.04.042
11. Liang, T.; Zhang, S.; Wang, L.; Kung, H-T.; Wang, Y.; Hu, A.; Ding, S. Environmental biogeochemical behaviors of rare earth elements in soil–plant systems. Environ. Geochem. Health. **2005**, 27, 301–311. https://doi.org/10.1007/s10653-004-5734-9
12. Adeel, M.; Lee, J.Y.; Zain, M.; Rizwan, M.; Nawab, A.; Ahmad, M.A.; Shafiq, M.; Yi, H., Jilani, G.; Javed, R.; Horton, R.; Rui, Y.; Tsang, D.C.W.; Xing, B. Cryptic footprints of rare earth elements on natural resources and living organisms. Environ. Int. **2019**, 127, 785-800. https://doi.org/10.1016/j.envint.2019.03022.
13. Turra, C. Sustainability of rare earth elements chain: from production to food-a review. Int. J. Environ. Health. Res. **2017**, 28, 23-42. https://doi.org/10.1080/09603123.2017.1415307
14. Gwenzi, W.; Mangori, L.; Danha, C.; Chaukura, N.; Dunjana, N.; Sanganyadoe, E. Sources, behaviour, and environmental and human health risks of high technology rare earth elements as emerging contaminants. Sci. Total Env. **2018**, 636, 289-313. https://doi.org/10.1016/j.scitotenv.2018.04.235.
15. Tommasi, F.; Thomas, P. J.; Pagano, G.; Perono, G.A.; Oral, R.; Lyons, D.M.; Toscanesi, M.; Trifuoggi, M. Review of rare earth elements as fertilizers and feed additives: a knowledge gap analysis. Arch. Environ. Contam. Toxicol. **2021**, 81:531–540. https://doi:10.1007/s00244-020-00773-4.

Preprints.org (www.preprints.org) | NOT PEER-REVIEWED | Posted: 19 March 2024 doi:10.20944/preprints202403.1161.v1

16. Rim, K.T.; Koo, K.H.; Park, J.S. Toxicological evaluations of rare earths and their health impacts to workers: a literature review. Saf. Health Work. **2013**, 4, 12-26. http://dx.doi.org/10.5491/SHAW.2013.4.1.12
17. Malhotra, N.; Hsu, H-S.; Liang, S-T.; Roldan, M.J.M.; Lee, J-S.; Ger, T-R.; Hsiao, C-D. An update review of toxicity effect of the rare earth elements (REEs) on aquatic organisms. Animals. **2020**, 10, 1663. https://doi:103390/ani10091663.
18. Kumar, S.; Prakash, R.; Singh, V.K. Synthesis, characterization, and applications of europium oxide: a review. Rev. Adv. Sci. Eng. **2015**, 4, 247-257. https://doi:10.1166/rase.2015.1102
19. Silva, R.; Chojnacki, J.; Falcão, E.H.; Alves, S. New coordination polymers based on a V-shaped ligand and lanthanides: Structural description and symmetry-luminescence correlation using europium as a probe. J. Lumin. **2017**, 182, 29-38. https://doi.org/10.1016/j.jlumin.2016.09.057.
20. Avila, J.N.; Ireland, T.R.; Lugaro, M.; Gyngard, F.; Zinner, E.; Cristallo, S.; Holden, P.; Rauscher, T. Europium s-process signature at close-to-solar metallicity in stardust sic grains from asymptotic giant branch stars. Astrophysic. J. Lett. **2013**, 768:L18. http://doi:10.1088/2041-8205/768/I/L18.
21. Trifuoggi, M.; Pagano, G.; Guida, M.; Palumbo, A.; Siciliano, A.; Gravina, M.; lyons, D.M.; Burié, P.; Levak, M.; Thomas, P.J.; Giarra, A.; Oral, R. Comparative toxicity of seven rare earth elements in sea urchin early life stages. Enviro. Sci. Poll. Res. **2017**, 24, 20803-20810. http://doi.10.1007/s11356-017-9658-1
22. Bollu, V.S.; Nethi, S.K.; Dasari, R. K.; Rao, S.S.N.; Misra, S.; Patra, C.R. Evaluation of in vivo cytogenetic toxicity of europium hydroxide nanorods (EHNs) in male and female Swiss albino mice. Nanotoxicol. **2016**, 10, 413-425. http://doi:10.3109/17435390.2015.1073398
23. Zhuang, W. Q.; Fitts, J. P.; Ajo-Franklin, C. M.; Maes, S.; Alvarez-Cohen, L.; Hennebel, T. Recovery of critical metals using biometallurgy. Curr. Opin. Biotechnol. **2015**, 33, 327-335. http://doi:10.1016/j.copbio.2015.03.019
24. Maleke, M.; Valverde, A.; Vermeulen, J. G.; Cason, E.; Gomez-Arias, A.; Moloantoa, K.; Coetsee-Hugo, L.; Swart, H.; Heerden, E.; Castillo, J. Biomineralization and bioaccumulation of europium by a thermophilic metal resistant bacterium. Front. Microbiol. **2019**, 10, 1-10. http://doi:10.3389/fmicb.2019.00081
25. Das, N.; Das, D. Recovery of rare earth metals through biosorption: an overview. J. Rar. Eart. **2013**, 31, 933-943. https://doi.org/10.1016/S1002-0721(13)60009-5
26. Furuhashi, Y.; Honda, R.; Noguchi, M.; Hara-Yamamura, H.; Kobayashi, S.; Higashimine, K.; Hasegawa, H. Optimum conditions of pH, temperatura and preculture for biosorption of europiu by microalgae *Acutodesmus acuminatus*. Biochen. Engin. J. **2019**, 143, 58-64. https://doi.org/10.1016/j.bej.2018.12.007
27. Jena, A.; Pradhan, S.; Mishra, S.; Sahoo, N.K. Evaluation of europium biosorption using *Deinococcus radiodurans*. Environ. Process. **2021**, 8, 251-265. https://doi.org/10.1007/s40710-020-00479-8
28. Philip, L.; Iyengar, L.; Venkobachar, C. Biosorption of U, La, Pr, Nd, Eu, and Dy by *Pseudomonas aeruginosa*. J. Ind. Microbiol. Biotechmol. **2000**, 25, 1-7. https://doi.org/10.1038/sj.jim.7000026
29. Liang, J.; Li, L.; Song, W. Improved Eu(III) immobilization by *Cladosporium sphaerospermum* induced by low-temperature plasma. J. Radioanal. Nuc. Chem. **2018**, 316, 963-970. https://doi.org/10.1007/s10967-018-5751-2
30. Arunraj, B.; Sathvika, T.; Rajesh, V.; Rajesh, N. Cellulose and *Saccharomyces cerevisiae* embark to recover europium from phosphor powder. ACS. Omega. **2019**, 4, 940-952. https://doi:10.1021/acsomega.8b02845
31. Kozai, N.; Skamoto, F.; Tanaka, K.; Ohnuki, T.; Satoh, T.; Kamiya, T.; Grambow, B. Complexation of Eu(III), Pb(II) and U(VI) with a *Paramecium* glycoprotein: microbial transformation of heavy elements in the aquatic environment. Chemosphere. **2018**, 196, 135-144. https://doi.org/10.1016/j.chemosphere.2017.12.154
32. Bonnet, J-L.; Dusser, M.; Bohatier, J.; Laffosse, J. Cytotoxicity assessment of three therapeutic agents, cyclosporine-A, cisplatin and doxorubicin, with the ciliated protozoan *Tetrahymena pyriformis*. Res. Microbiol. 2003, 154, 375-385. https://doi:10.1016/S0923-2508(03)00085-8
33. Diaz, S.; Martin-Gonzalez, A.; Gutierrez, J.C. Evaluation of heavy metal acute toxicity and bioaccumulation in soil ciliated protozoa. Environ. Int. **2006**, 32, 711-717. https://doi:10.1016/j.envint.2006.03.004
34. Diaz, S.; Martin-Gonzalez, A.; Cubas, L.; Ortega, R.; Amaro, F.; Rodriguez-Martin, D.; Gutierrez, J.C. High resistance of *Tetrahymena thermophila* to paraquat: mitocondrial alterations, oxidative stress and antioxidant genes expression. Chemosphere. **2016**, 144, 909-917. http://dx.doi.org/10.1016/j.chemosphere.2015.09.010
35. Gutierrez, J.C.; Martin-Gonzalez, A.; Diaz, S.; Ortega, R. Ciliates as a potential source of cellular and molecular biomarkers/biosensors for heavy metal pollution. Eu. J. Protistol. **2003**, 39, 461-467. https://doi.org/10.1078/0932-4739-00021
36. Nilsson, L.R. 1989. Dose- and pH-dependent effects of chloroquine on *Tetrahymena*. Eu. J. Protistol. 1989, 24, 297-307. https://doi.org/10.1016/S0932-4739(89)80001-X
37. Romero, I.; De Francisco, P.; Gutierrez, J.C.; Martin-Gonzalez, A. Selenium cytotoxicity in *Tetrahymena thermophila*: new clues about its biological effects and cellular resistance mechanisms. Sci. Total Environ. **2019**, 671, 850-865. https://doi.org/10.1016/j.scitotenv.2019.03.115
38. Sauvant, N.P.; Pepin, D.; Piccinni, E. *Tetrahymena pyriformis*: a tool for toxicological studies. A review. Chemosphere. **1999**, 38, 1631-1669. https://doi.org/10.1016/S0045-6535(98)00381-6

39. Eisen, J.A.; Coyne, R.S.; Wu, M.; Wu, D.; Thiagarajan, M.; et al. Macronuclear genome sequence of the ciliate *Tetrahymena thermophila*, a model eukaryote. PLoS Biol. **2006**, 4(9): e286. https://doi:10.1371/journal.pbio.0040286
40. De Francisco, P.; Martin-Gonzalez, A.; Turkewitz, A.P.; Gutierrez, J.C. Genome plasticity in response to stress in *Tetrahymena thermophila*: selective and reversible chromosome amplification and paralogous expansion of metallothionein genes. Environ. Microbiol. **2018**, 20, 2410-2421. https://doi:10.1111/1462-2920.14251
41. Baranyi, J.; Roberts, T.A. A dynamic approach to predicting bacterial growth in food. Int. J. Food Microbiol. **1994**, 23, 277-294. https://doi.org/10.1016/0168-1605(94)90157-0
42. Rodriguez-Martin, D.; Murciano, A.; Herraiz, M.; De Francisco, P.; Amaro, F.; Gutierrez, J.C.; Martin-Gonzalez, A.; Diaz, S. Arsenate and arsenite differential toxicity in *Tetrahymena thermophila*. J. Hazard Mater. **2022**, 431, 128532. https://doi.org/10.1016/j.jhazmat.2022.128532
43. Garner, D.L.; Johnson, L.A.; Yue, S.T.; Roth, B.L.; Haugland, R.P. Dual DNA staining assessment of bovine sperm viability using SYBR-14 and propidium iodide. J. Androl. **1994**, 15, 620-629. https://doi.org/10.1002/j.1939-4640.1994.tb00510.x
44. Eruslanov, E.; Kusmartsev, S. Identification of ROS using oxidized DCFDA and flowcytometry. Methods Mol. Biol. Humana Press Inc. **2010**, pp. 57-72. https://doi.org/10.1007/978-1-60761-411-1_4
45. Cubas-Gaona, L.L.; De Francisco, P.; Martin-Gonzalez, A.; Gutierrez, J.C. *Tetrahymena* glutathione peroxidase family: a comparative analysis of these antioxidant enzymes and differential gene expression to metals and oxidizing agents. Microorganisms. **2020**, 8, 1008. https://doi:10.3390/microorganisms8071008
46. Dentler, W. Fixation of *Tetrahymena* cells for electron microscopy. Methods Cell Biol. **2000**, 62, 323-331. https://doi:10.1016/s0091-679x(08)61540-x
47. Borges, A.; Tsai, S.M.; Gomes-Caldas, D.G. Validation of reference genes for RT-qPCR normalization in common bean during biotic and abiotic stresses. Plant Cell Rep. **2012**, 31, 827-838. https://doi.org/10.1007/s00299-011-1204-x
48. Larionov, A.; Krause, A.; Miller, W. A standard curve-based method for relative real time PCR data processing. BMC Bioinf. **2005**, 6, 1–16. https://doi.org/10.1186/1471-2105-6-62.
49. Gutierrez, J.C.; Amaro, F.; Diaz, S.; De Francisco, P.; Cubas, L.L.; Martin-Gonzalez, A. Ciliate metallothioneins: unique microbial eukaryotic heavy-metal-binder molecules. J. Biol. Inorg. Chem. **2011**, 16, 1025-1034. https://doi.10.1007/s00775-011-0820-9
50. Díaz, S.; Amaro, F.; Rico, D.; Campos, V.; Benítez, L.; Martín-González, A.; Hamilton, E.P.; Orias, E.; Gutiérrez, J.C. *Tetrahymena* metallothioneins fall into two discrete subfamilies. PLoS One **2007**, 2 (3), e291. https://doi:10.1371/journal.pone.0000291
51. Gallego, A.; Martin-Gonzalez, A.; Ortega, R.; Gutierrez, J.C. Flow cytometry assessment of cytotoxicity and reactive oxygen species generation by single and binary mixtures of cadmium, zinc and copper on populations of the ciliated protozoon *Tetrahymena thermophila*. Chemosphere. **2007**, 68, 647-661. https//doi:10.1016/j.chemosphere.2007.02.031
52. Pallares, R.M.; An, D.D.; Hebert, S.; Faulkner, D.; Loguinov, A.; Proctor, M.; Villalobos, J.A.; Bjornstad, k.A.; Rosen, C.J.R.; Vulpe, C.; Abergel, R.J. Multidimensional genome-wide screening in yeast provides mechanistic insights into europium toxicity. Metallomics. **2021**, 13, mfab061. https://doi.org/10.1093/mtomcs/mfab061
53. Tai, P.; Zhao, Q.; Su, D.; Li, P.; Stagnitti, F. Biological toxicity of lanthanide elements on algae. Chemosphere. **2010**, 80, 1031-1033. https://doi:10.1016/j.chemosphere.2010.05030
54. Kurvet, I.; Juganson, K.; Vija, H.; Sihtmae, M.; Blinova, I.; Syvertsen-Wiig, G.; Kahru, A. Toxicity of nine (doped) rare earth metal oxides and respective individual metals to aquatic microorganisms *Vibrio fischeri* and *Tetrahymena thermophila*. Materials. **2017**, 10, 754. https://doi:10.3390/ma10070754
55. Wang, Y.; Zhang, M.; Wang, X. Population growth responses of *Tetrahymena shanghaiensis* in exposure to rare earth elements. Biol. Trace Elem. Res. **2000**, 75, 265-275. https;//doi:10.0163-4984/00/7501-3-0265
56. Maleke, M.; Valverde, A.; Gomez-Arias, A.; Cason, E.D.; Vermeulen, J-G.; Coetsee-Hugo, L.; Swart, H.; van Heerden, E.; Castillo, J. Anaerobic reduction of europium by a *Clostridium* strain as a strategy for rare earth biorecovery. Scin. Rep. **2019**, 9, 14339. https://doi.org/10.1038/s41598-019-50179-z
57. Zhao, H.; Osborne, O.J.; Lin, S.; Ji, Z.; Damoiseux, R.; Wang, Y.; Nel, A.E.; Lin, S. Lanthanide hydroxide nanoparticles induce angiogenesis via ROS-sensitive signaling. Small. **2016**, 12, 4404-4411. https://doi:10.1002/smll.201600291
58. Brown, M.B.; Forsythe, A.B. Robust tests for the equality of variances. J. Amer. Statis. Assoc. **1974**, 69, 364-367. https://doi:10.1080/01621459.1974.10482955
59. Gutierrez, J.C.; Martin-Gonzalez, A.; Diaz, S.; Amaro, F.; Ortega, R.; Gallego, A.; De Lucas, M.P. Ciliates as cellular tools to study the eukaryotic cell-heavy metal interactions. In Heavy Metal Pollution. Nova Science Publishers, Inc. **2008**, pp. 1-44. ISBN: 978-1-60456-899-8.

60. Sheng, Y.; Abreu, I.A.; Cabelli, D.E.; Maroney, M.J.; Miller, A-F.; Teixeira, M.; Valentine, J.S. Superoxide dismutases and superoxide reductases. Chem. Rev. **2014**, 114, 3854-3918. https://dx.doi.org/10.1221/cr4005296
61. Wei, W.; Wang, H.; Jiang, C. Spectrofluorimetric determination of superoxide dismutase using a europium-tetracycline probe. Spectrochim. Acta Part A. **2008**, 70, 389-393. https://doi:10.1016/j.saa.2007.10.046
62. De Francisco, P.; Melgar, L.M.; Diaz, S.; Martin-Gonzalez, A.; Gutierrez, J.C. The *Tetrahymena* metallothionein gene family: twenty-one new cDNAs, molecular characterization, phylogenetic study and comparative analysis of the gene expression under different abiotic stressors. BMC Genomics. **2016**, 17:346. https://doi:10.1186/s12864-016-2658-6
63. De Francisco, P.; Martin-Gonzalez, A.; Turkewitz, A.P.; Gutierrez, J.C. Extreme metal adapted, knockout and knockdown strains reveal a coordinated gene expression among different *Tetrahymena thermophila* metallothionein isoforms. PloS One. **2017**, 12(12):e0189076. https://doi.org/10.1371/journal.pone.0189076
64. Wang, Q.; Xu, J.; Zhu, Y.; Chai, B.; Liang, A.; Wang, W. Lanthanum (III) impacts on metallothionein MTT1 and MTT2 from *Tetrahymena thermophila*. Biol. Trace Elem. Res. **2011**, 143, 1808-1818. https://doi:10.1007/s12011-011-9004-2
65. Geng, M-J.; Liang, S-X.; liu, W.; Jin, Y. Quantification of metallothioneins in the earthworm by lomefloxacin-europium(III) fluorescent probe. Environ. Sci. Processes Impacts. **2014**, 16, 1923-1929. https://doi:10.1039/c4em00076e
66. Silber, H.B.; Paquette, S.J. Complexes of lanthanide ions with amino acids, nucleotides, and other ligands of biological interest in solution. In Metal ions in biological systems. The lanthanides and their Interrelations with biosystems. **2003**, Vol. 40. pp. 799. Ed. Sigel, A, and Sigel, H. CRC Press. ISBN 13: 978-0-8247-4245-4
67. Lafita-Navarro, M.C.; Conacci-Sorrell, M. Nucleolar stress: from development to cancer. Semin. Cell Develop. Biol. **2023**, 136, 64-74. https://doi.org/10.1016/j.semcdb.2022.04.001
68. Bahadori, M. New insights into connection of nucleolar functions and cancer. Tanaffos. **2019**, 18, 173-179. ISSN: 1735-0344.
69. Weeks, S.; Metge, B.J.; Samant, R.S. The nucleolus: a central response hub for the stressors that drive cancer progression. Cell. Mol. Life Sci. **2019**, 76, 4511-4524. https://doi.org/10.1007/s00018-019-03231-0
70. Neuburger, M.; Herget, G.W.; Plaumann, L.; Falk, A.; Schwab, H.; Adler, C-P. Change in size, number, and morphology of the nucleoli in human hearts as a result of hyperfunction. Pathol. Res. Pract. **1998**, 194, 385-390. https://doi.org/10.1016/S0344-0338(98)80028-9
71. MacMillan, G.A.; Clayden, M.G.; Chetelat, J.; Richardson, M.C.; Ponton, D.E.; Perron, T.; Amyot, M. Environmental drivers of rare earth element bioaccumulation in freshwater zooplankton. Environ. Sci. Technol. **2019**, 53, 1650-1660. https://doi:10.1021/acs.est.8b05547
72. Henne, W.M.; Reese, M.L.; Goodman, J.M. 2018. The assembly of lipid droplets and their roles in challenged cells. EMBO J. **2018**, 37:e98947. https://doi:10.15252/embj.201898947
73. Singh, R.; Kaushik, S.; Wang, Y.; Xiang, Y.; Novak, I.; Komatsu, M.; Tanaka, K.; Cuervo, A.M.; Czaja, M.J. 2009. Autophagy regulates lipid metabolism. Nature. **2009**, 458,1131-1135. https://doi:10.1038/nature07976
74. Cui, L.; Liu, P. Two types of contact between lipid droplets and mitochondria. Front. Cell. Dev. Biol. **2020**, 8:618322. https://doi:10.3389/fcell.2020.618322
75. Amen, T.; Kaganovich, D. Dynamic droplets: the role of cytoplasmic inclusions in stress, function, and disease. Cell. Mol. Life Sci. **2015**, 72, 401-415. https://doi:10.1007/s0008-014-1740-y
76. Rajakumar, S.; Nachiappan, V. Lipid droplets alleviate cadmium-induced cytotoxicity in *Saccharomyces cerevisiae*. Toxicol. Res. **2017**, 6, 30-41. https://doi:10.1039/c6tx00187d
77. Kennedy, D.C.; Lyn, R.K.; Pezacki, J.P. Cellular lipid metabolism is influenced by the coordination environment of copper. J. Am. Chem. Soc. **2009**, 131, 2444–2445. https://doi.org/10.1021/ja809451w
78. Moron, A.; Martin-Gonzalez, A.; Diaz, S.; Gutierrez, J.C.; Amaro, F. Autophagy and lipid droplets are a defense mechanism against toxic copper oxide nanotubes in the eukaryotic microbial model *Tetrahymena thermophila*. Sci. Total Environ. **2022**, 847, 157580. http://dx.doi.org/10.1016/j.scitotenv.2022.157580
79. Jiang, M.; Ohnuki, T.; Utsunomiya, S. Biomineralization of middle rare earth element samarium in yeast and bacteria systems. Geomicrobiol. J. **2018**, 35, 375-384. https://doi.org/10.1080/01490451.2017.1377320
80. Nadella, S.; Sahoo, J.; Subramanian, P.S.; Sahu, A.; Mishra, S.; Albrecht, M. Sensing of phosphates by using luminescent Eu(III) and Tb(III) complexes: application to the microalgal cell *Chlorella vulgaris*. Chem. Eur. J. **2014**, 20, 1-8. https://doi:10.1002/chem.201304664
81. Jiang, M.; Ohnuki, T.; Kozai, N.; Tanaka, K.; Suzuki, Y.; Sakamoto, F.; Kamiishi, E.; Utsunomiya, S. Biological nano-mineralization of Ce phosphate by *Saccharomyces cerevisiae*. Chem. Geol. **2010**, 277, 61-69. https://doi:10.1016/j.chemgeo.2010.07.010

doi:10.20944/preprints202403.1161.v1

82. Jiang, M.; Ohnuki, T.; Kozai, N.; Tanaka, K.; Kozai, N.; Kamiishi, E.; Utsunomiya, S. Post-adsorption process of Yb phosphate nano-particle formation by *Saccharomyces cerevisiae*. Geochim. Cosmochim. Acta. **2012**, 93, 30-46. https://doi:10.1016/j.gca.2012.06.016
83. De Francisco, P.; Amaro, F.; Martin-Gonzalez, A.; Serrano, A.; Gutierrez, J.C. Quantitative proteomic analyses of a Pb-adapted *Tetrahymena thermophila* strain reveal the cellular strategy to Pb(II) stress including lead biomineralization to chloropyromorphite. Sci. Total Environ. **2023**, 891, 164252. http://dx.doi.org710.1016/j.scitotenv.2023.164252